Theoretical Chemistry Accounts (2021) 140:26
https://doi.org/10.1007/s00214-021-02720-5

REGULAR ARTICLE

Nuclear magnetic resonance parameters in Zn_2, Cd_2 and Hg_2 dimers: relativistic calculations

Katarzyna Jakubowska[1] · **Magdalena Pecul**[1]

Received: 23 October 2019 / Accepted: 16 January 2021 / Published online: 23 February 2021

Abstract
The potential energy curves and the NMR properties: nuclear spin–spin coupling constants and nuclear shielding constants have been calculated for Zn_2, Cd_2 and Hg_2 dimers using density functional theory. The calculations have been carried out using the relativistic four-component Dirac–Coulomb Hamiltonian, and, in the case of energy curves, also relativistic effective core potentials. In case of NMR parameters, the relativistic effects turned out to be critically important even for the lightest dimer, Zn_2. The importance of the spin–orbit coupling depends on the internuclear distance: these effects tend to be significant for short internuclear distances.

Keywords Nuclear magnetic resonance · Spin–spin coupling constant · Shielding constant · Relativistic calculations · Dirac–Coulomb Hamiltonian · Group 12 dimers

1 Introduction

Closed-shell van der Waals metal dimers are of scientific interest [1–17] for their own sake, due to the possibility of laser applications (in analogy with the homo- and heteroatomic noble gas excimers and exciplexes [18]), and as the smallest metal clusters, providing information relevant for the study of condensation processes. The Zn_2, Cd_2 and Hg_2 series is especially interesting due to atypical properties of mercury—the only metal liquid in room temperature and under atmospheric pressure—which are attributed to the relativistic effects. Mercury has an additional aspect attracting attention of computational chemistry: the nucleus of ^{199}Hg has a 1/2 spin and relatively high abundance, making ^{199}Hg NMR a suitable tool for investigation of mercury complexes. We explore both aspects of Zn_2, Cd_2 and Hg_2 dimers in this contribution: energetics and nuclear magnetic resonance properties.

Our main focus is NMR properties of the dimers under study: nuclear shielding constants, sensitives probes of van der Waals interactions, and the nuclear spin–spin coupling constants transmitted through these interactions. However, in order to choose an appropriate exchange-correlation functional for the calculation of NMR properties in these van der Waals complexes, the potential energy curves have been first investigated by a variety of methods. The results have been compared with experiment and previous computational studies [1–7, 9, 12–15, 19].

The present study is carried out using relativistic four-component Dirac–Coulomb Hamiltonian, which allows us to take into account the relativistic effects in the most complete way available for NMR properties. (It should be kept in mind, however, that this is not a fully relativistic Hamiltonian and that the first-order Breit correction to the missing terms may quite significantly contribute to the calculated NMR properties of mercury [20]). We also compare the potential energy curves calculated using the four-component Hamiltonian with the results of calculations carried out by means of one-component Hamiltonian with effective core potentials. Another methodological issue under consideration is the performance of different exchange correlation density functionals in comparison with the coupled cluster calculations.

The contribution is organized as follows. First, we describe the computational details. Afterwards, the calculated potential energy curves and NMR properties are presented. The paper is concluded with a summary.

✉ Katarzyna Jakubowska
kjakubowska@chem.uw.pl

Magdalena Pecul
mpecul@chem.uw.edu.pl

[1] Faculty of Chemistry, University of Warsaw, Pasteura 1, 02-093 Warsaw, Poland

2 Computational details

2.1 Four-component calculations of potential energy curves

The four-component Dirac–Kohn–Sham calculations of potential energy curves have been carried out with the ReSpect [21] program. Uncontracted triple-ζ Dyall's basis set [22, 23] (dyall.vtz) has been applied together with a variety of exchange-correlation functionals: BLYP [24, 25], B3LYP [25–28], BHLYP [24] PBE [29], PBE0 [30] and PBE0-50 (PBE0 with increased to 50% exact exchange admixture). Moreover, four-component Hartree–Fock calculations have been performed. Unfortunately, ReSpect does not support ghost atoms and, thus, basis set superposition error (BSSE) could not have been estimated.

The potential energy curves for dimers under consideration have been also computed with the use of coupled-cluster method (CCSD and CCSD(T) models), four-component Dirac–Coulomb Hamiltonian [31] and DZP basis set [32–34] by means of DIRAC [35]. Relatively small DZP basis set has been chosen in order to limit the computational cost as coupled cluster calculations are highly memory- and time-demanding. In all these cases finite Gaussian-type nuclear charge distribution model has been applied.

2.2 One-component ECP calculations of potential energy curves

The effective core potential results have been obtained using the Gaussian 09 program [36]. The following effective core potentials have been employed: MWB28 for zinc and cadmium [37], MWB60 for mercury [37]. Two electronic structure methods have been applied DFT together with PBE0, B3LYP and CAM-B3LYP [38] functionals and CCSD(T). BSSE has been taken into account with counterpoise correction [39].

2.3 Four-component calculations of NMR parameters

For the following calculations of NMR parameters four-component Dirac–Kohn–Sham Hamiltonian, PBE0 functional and uncontracted triple-ζ Dyall's basis set have been applied. Some calculations have also been performed with the use of PBE0-50 functional. The calculations have been performed with ReSpect programme, using restricted magnetically balanced basis [40–42]. For comparison, also four-component calculations with spin–orbit interactions switched off and nonrelativistic calculations have been carried out. In the case of the nonrelativistic computations the speed of light has been scaled to 50.0 a.u. and in case of the four-component calculations without spin–orbit effects the spin–orbit operators have been scaled by a factor 0 (as implemented in ReSpect).

3 Results and discussion

3.1 Potential energy curves

3.1.1 Four-component calculations of potential energy curves

The potential energy curves (scaled to binding energy curves—shifted so as to give 0 at infinite internuclear separation) calculated using DKS-DFT with different exchange-correlation functionals are shown in Fig. 1. In order to compare the obtained results with experiment and literature computational results (coupled cluster calculations with Dirac–Coulomb Hamiltonian, denoted DCH-CCSD(T)), the values of R_e and D_e have been presented in Table 1. Unfortunately, in case of DKS calculations BLYP, B3LYP and BHLYP functionals do not even produce a minimum and, thus, they are not further considered. The performance of PBE0 and PBE0-50 functionals seems to be satisfactory, although obviously inferior to CCSD(T). In the case of Zn_2 and Cd_2 the calculated values of R_e are too low as compared to the experiment and the literature CCSD(T) values. There is a good agreement between the calculated values of R_e for the Hg_2. In all cases the values of D_e calculated with PBE0 are 20–30% higher than those calculated with PBE0-50, which brings them further from the experiment in the case of Zn_2 and Cd_2, but closer for Hg_2. To sum up, PBE0 and PBE0-50 seem to handle relatively correctly the energetics of the dimers under study, and are superior in this respect to PBE and much superior to the functionals from the BLYP family (Fig. 1).

All three systems under investigation are weakly bound van der Waals complexes and, therefore, basis set superposition error should be taken into consideration [43]. In case of the DFT calculating counterpoise correction [39], which can be estimated by performing subsystem calculations using ghost atoms carrying basis sets of the full system, might be somehow problematic. From this reason and the fact that ReSpect program does not enable the use of ghost atoms, we do not take BSSE into account in this case. In the next subsection we discuss how the introduction of CP correction influences the potential energy curves in case of ECP calculations.

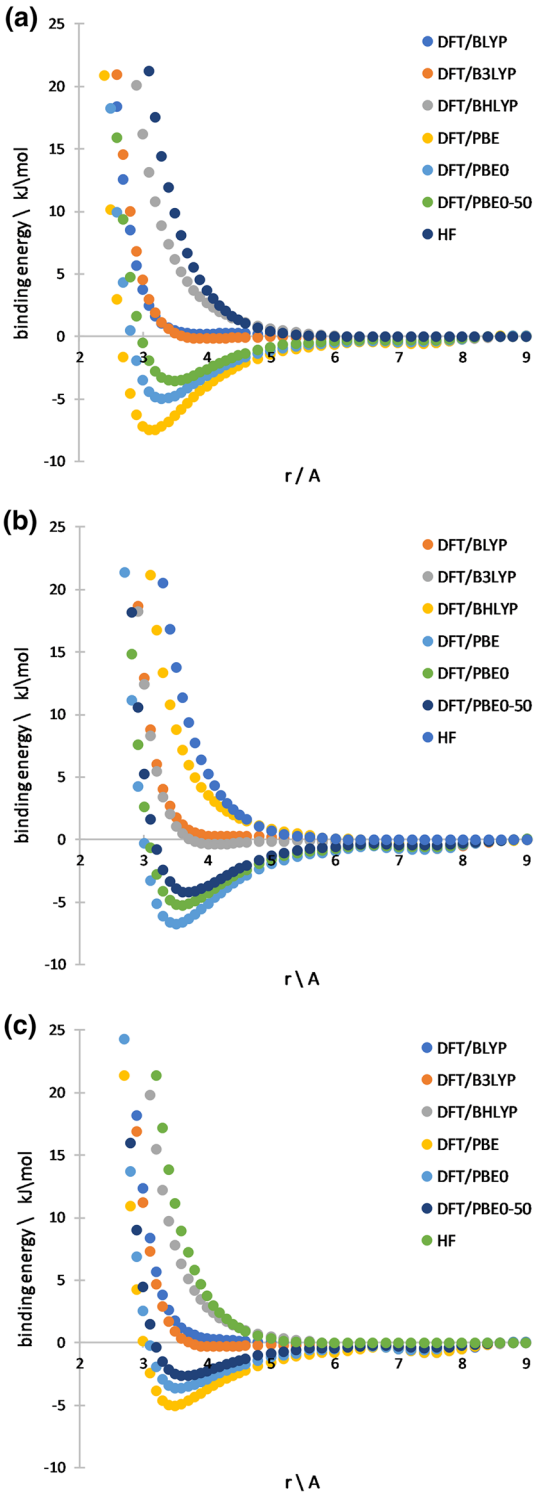

Fig. 1 The Zn_2 (**a**) , Cd_2 (**b**) and Hg_2 (**c**) potential energy curves calculated with DKS. The curves were shifted so as to give 0 at infinite internuclear separation

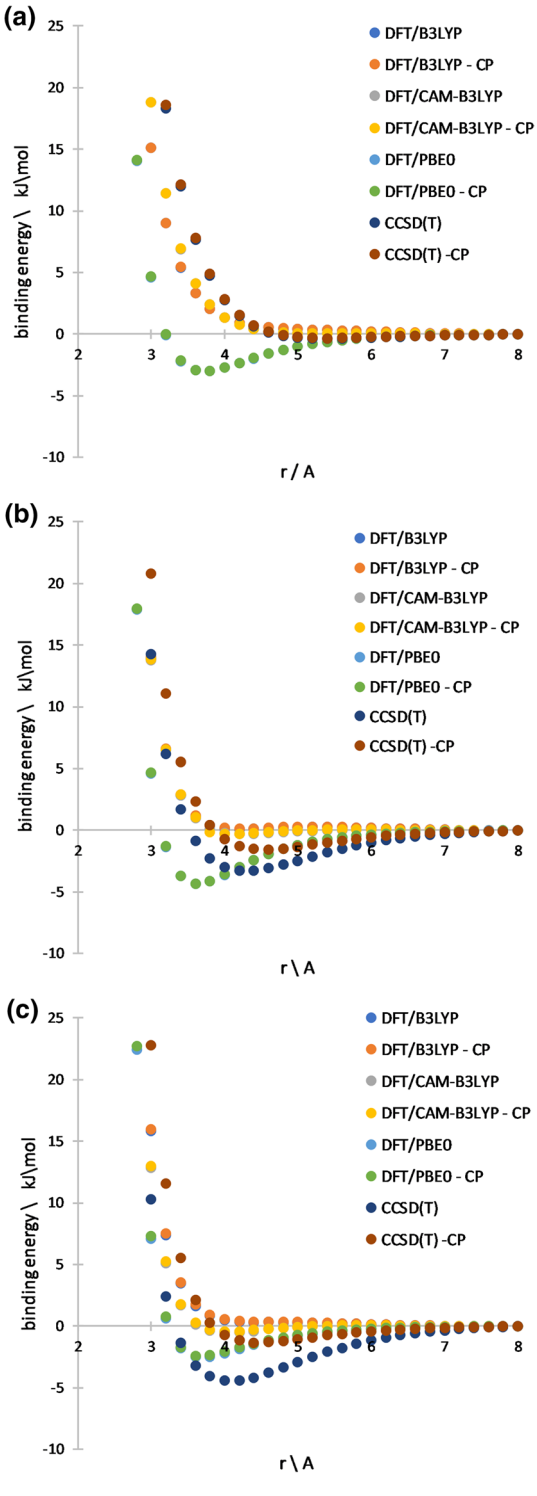

Fig. 2 The Zn_2 (**a**) , Cd_2 (**b**) and Hg_2 (**c**) potential energy curves calculated with ECPs. The curves were shifted so as to give 0 at infinite internuclear separation

Table 1 Comparison of the calculated values of R_e and D_e with literature

	Zn_2		Cd_2		Hg_2	
	R_e [Å]	D_e [cm^{-1}]	R_e [Å]	D_e [cm^{-1}]	R_e [Å]	D_e [cm^{-1}]
Experiment	4.19 [1]	279 [1]	4.07 [19]	330 [19]	3.63 [19]	380 [19]
DCH-CCSD(T) [16]	3.58	315.2	4.08	302.9	3.87	357.8
DKS[a]						
DFT/PBE	3.15	624	3.46	562	3.45	417
DFT/PBE0	3.33	415	3.56	437	3.52	300
DFT/PBE0-50	3.46	295	3.68	351	3.60	219
ECP						
DFT/PBE0	3.71	247	3.63	361	3.69	208
CCSD(T)	5.31	28	4.28	273	4.09	369
CCSD(T)-CP	5.31	28	4.60	127	4.43	108

[a]Values for BLYP, B3LYP, BHLYP, CAM-B3LYP have not been included, since these functionals either did not produce a minimum or it was extremely shallow (< 50 cm^{-1})

3.1.2 ECP calculations of potential energy curves

The potential energy curves calculated using ECPs are shown in Fig. 2. As it can be noticed in case of DFT the performance of PBE0 functional is also the most satisfactory as compared to the experiment. The B3LYP functional does not produce a minimum, whereas the minima produced by the CAM-B3LYP functional are much too shallow and the minimum energy interatomic separations are too long.

The ECP-CCSD(T) results are extremely poor in case of Zn_2 dimer. It probably results from the use of MWB28 ECP, which means that only 2 electrons are treated explicitly. In case of both Cd_2 and Hg_2 the results are in better agreement with the experiment; however, their quality is not better than the quality of the DFT/PBE0 results.

It is worth mentioning how BSSE affects the results. The comparison of the values calculated with and without counterpoise correction shows that the differences in case of the DFT results are negligible. As far as CCSD(T) results are concerned, the minima become more shallow and move to higher interatomic distances, which makes the agreement with experiment much worse.

In cases such as the dimers under consideration, it is often recommended to perform DFT calculation with a functional using Coulomb-attenuating method. Comparison of the results obtained either with CAM-B3LYP or B3LYP functional shows that the use of Coulomb-attenuating method does indeed improve the quality of the results. However, the improvement is subtle and the performance of PBE0 functional is still much more satisfactory. In particular, CAM-B3LYP gives very shallow minima for Cd_2 (23 cm^{-1}) and Hg_2 (42 cm^{-1}) and it does not produce a minimum for Zn_2 at all.

3.2 Nuclear shielding constants

On the basis of the results for potential energy curves, we have selected PBE0 correlation-exchange functional for NMR calculations. For comparison, some calculations have also been performed with PBE0-50 functional. Diagrams showing dependencies of the calculated nuclear shielding constants for Zn_2, Cd_2 and Hg_2 on interatomic distances can be found in Fig. 3.

As it turns out relativistic effects are essential in calculations of shielding constants for all three dimers under consideration. Contribution of relativity changes only for very small r values, for $r > 3.0$ it is almost constant: ca. 7% for σ_{Zn}, ca. 16% for σ_{Cd} and ca. 40% for σ_{Hg}.

As far as contribution of spin–orbit effects to relativistic effects is concerned, it is clear from the diagrams that there is no point in calculating nuclear shielding constants, especially at lower interatomic separations, without including spin–orbit effects. At small interatomic distances, the contribution of spin–orbit effects to relativistic effects on the whole is negative and can be even over 300%. With the increase in r parameter it rises and becomes positive. It becomes practically constant for the distances larger than 6.0 Å and it is at the level of 0.85% for Zn_2, 1.23% for Cd_2 and 2.43% for Hg_2.

Comparison of four-component relativistic values of shielding constants for Zn_2, Cd_2 and Hg_2 calculated with either PBE0-50 or PBE0 functional shows that the difference in the values does not exceed 2% and shape of the r-dependency does not change.

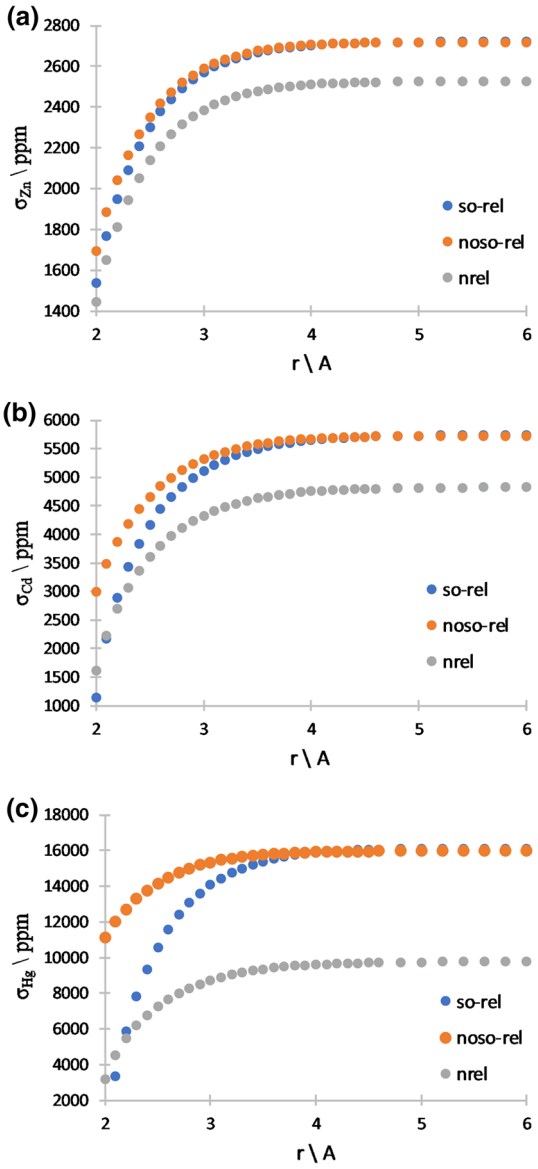

Fig. 3 Dependence of the nuclear shielding constants: **a** σ_{Zn}, **b** σ_{Cd} and **c** σ_{Hg} on the interatomic distance, r

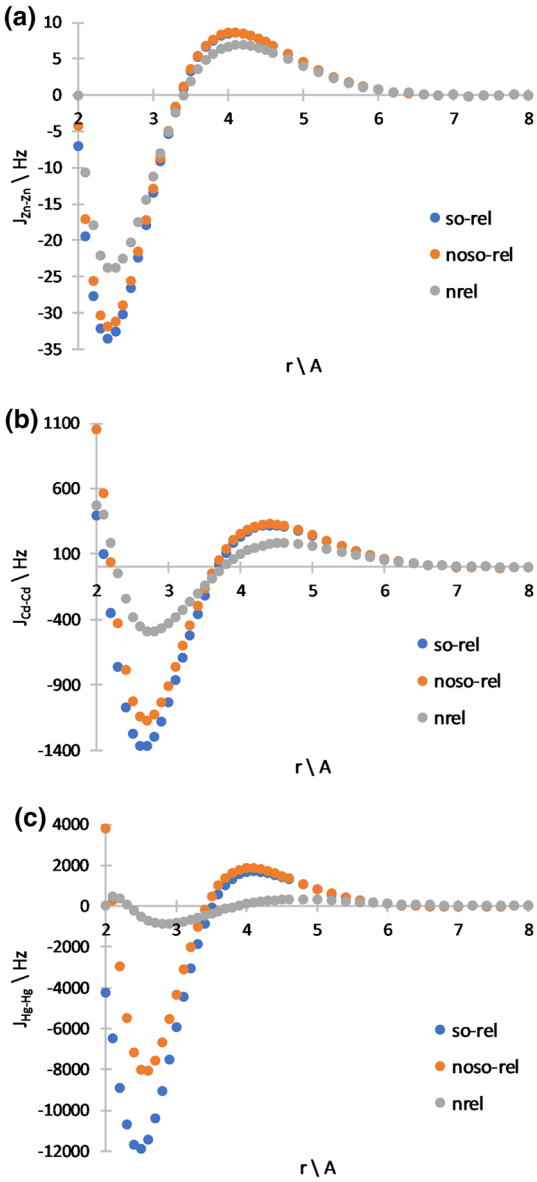

Fig. 4 Dependence of the spin–spin coupling constants: **a** J_{Zn-Zn}, **b** J_{Cd-Cd} and **c** J_{Hg-Hg} on the interatomic distance, r

3.3 Nuclear spin–spin coupling constants

Diagrams of the nuclear spin–spin coupling constants calculated for Zn_2, Cd_2 and Hg_2 with changing interatomic distances are shown in Fig. 4. All three dependencies have a similar course with a minimum at about 2.4 - 2.7 Å and a maximum at about 4.1 - 4.6 Å. The only exception is the dependence of J_{Hg-Hg} that has been calculated with a non-relativistic method.

The influence of relativity turns out to be significant even for the lightest dimer, Zn_2. Relativistic contribution to the total value of the spin–spin constant decreases with the increase in the r value. It decreases from ca. 40% to ca. 5% for Zn_2, from over 90% to less than 10% for Cd_2 and from almost 100% to about 10% for Hg_2.

It can be noticed that spin–orbit effects play an important role only for small interatomic separations and they are negligible for larger distances. Spin–orbit effects constitute even over 20% for r smaller than 3.5 Å for Zn_2, 4.0 Å for Cd_2 and Hg_2. Moreover, they are less than 3 % for r larger than 4.2 Å for Zn_2, 5 Å for Cd_2 and 6.2 Å for Hg_2.

Comparison of four-component relativistic values of spin–spin coupling constants calculated for Zn_2, Cd_2 and Hg_2 with either PBE0 or PBE0-50 functional shows that, in contrast to the shielding constants, the difference in the

values can be even over 30% for larger r values, although the shape of the r-dependency does not change much visually.

4 Conclusions

We have studied potential energy curves of Zn_2, Cd_2 and Hg_2 dimers by means of the CCSD(T) and DFT methods with four-component Dirac–Coulomb Hamiltonian and one-component Hamiltonian with ECPs. After that nuclear magnetic shielding constants and nuclear spin–spin coupling constants were calculated at the DFT level. All the NMR calculations were carried out with Dirac–Coulomb Hamiltonian, and some of them were repeated with non-relativistic Hamiltonian. The conclusions are as follows:

- In the case of four-component DKS and one-component ECP DFT energy calculations for the dimers under consideration hybrid functionals from PBE0 family give satisfactory results as compared to the experiment, whereas hybrid functionals from B3LYP family perform very poorly.
- Including CP correction into ECP results for DFT energy calculations does not significantly improve the quality of the obtained values. It did not noticeably change either the depth or the location of the minimum energy.
- As far as computations of nuclear shielding constants are concerned, it is essential to incorporate relativistic effects even for the lightest dimer at all interatomic separations as relativistic effects are almost constant with change in r. In order to get accurate results at intermolecular distances around R_e the spin–orbit effects also need to be taken into account.
- Similar conclusions as for the shielding constants can be drawn for the spin–spin coupling constants. However, in this case relativistic effects decrease with the increase in interatomic distance.

Acknowledgements We acknowledge financial support from the Polish National Science Centre on the basis of the decision DEC-2014/15/B/ST4/05039.

Compliance with ethical standards

Conflict of interest The authors declare that they have no conflict of interest.

References

1. Czajkowski M, Koperski J (1999) Spectrochim Acta A 55(11):2221. https://doi.org/10.1016/S1386-1425(99)00020-7
2. Kunz CF, Hattig C, Hess BA (1996) Mol Phys 89:139. https://doi.org/10.1080/002689796174056
3. Munro LJ, Johnson JK, Jordan KD (2001) J Chem Phys 114:5545. https://doi.org/10.1063/1.1351877
4. Gaston N, Schwerdtfeger P (2006) Phys Rev B 74:024105. https://doi.org/10.1103/PhysRevB.74.024105
5. Pahl E, Figgen D, Thierfelder C, Peterson KA, Calvo F, Schwerdtfeger P (2010) J Chem Phys 132:114301. https://doi.org/10.1063/1.3354976
6. Flad HJ, Dolg M (1996) J Chem Phys 100:6147. https://doi.org/10.1021/jp952807x
7. Czuchaj E, Rebentrost F, Stoll H, Preuss H (1997) J Chem Phys 214:277. https://doi.org/10.1063/1.464326
8. Ruszczak M, Strojecki M, Krośnicki M, Lukomski M, Koperski J (2006) Optica Applicata 214:451
9. Urbańczyk T, Strojecki M, Krośnicki M, Kędziorski A, Żuchowski PS, Koperski J (2017) Int Rev Phys Chem 36:541. https://doi.org/10.1080/0144235X.2017.1337371
10. Strojecki M, Krośnicki M, Urbańczyk T, Pashov A, Koperski J (2015) Phys Rep 591:1. https://doi.org/10.1016/j.physrep.2015.06.004
11. Schwerdtfeger P, Wesendrup R, Moyano GE, Sadlej AJ, Greif J, Hensel F (2001) J Chem Phys 115:7401. https://doi.org/10.1063/1.1402163
12. Gaston N, Schwerdtfeger P, Saue T, Greif J (2006) J Chem Phys 124:044304. https://doi.org/10.1063/1.2139670
13. Kullie O (2014) J Chem Phys 140:024304. https://doi.org/10.1063/1.4859258
14. Yu M, Dolg M (1997) Chem Phys Lett 273:329. https://doi.org/10.1016/S0009-2614(97)00609-X
15. Pahl E, Figgen D, Borschevsky A, Peterson K, Schwerdtfeger P (2011) Theor Chem Acc 129(3–5):651. https://doi.org/10.1007/s00214-011-0912-1
16. Bučinský L, Biskupič S, Ilčin M, Lukeš V, Laurinc V (2009) J Comput Chem 30(1):65. https://doi.org/10.1002/jcc.21030
17. Schwerdtfeger P, Wesendrup R, Moyano G, Sadlej A, Greif J, Hensel F (2001) J Chem Phys 115(16):7401. https://doi.org/10.1063/1.1402163
18. Miller JC, Andrews L (1980) Appl Spectrosc Rev 16:1. https://doi.org/10.1080/05704928008081708
19. Czuchaj E, Rebentrost F, Stoll H, Preuss H (1996) Chem Phys Lett 255(1):203. https://doi.org/10.1016/0009-2614(96)00336-3
20. Seino J, Hada M (2010) J Chem Phys 132:17. https://doi.org/10.1063/1.3413529
21. ReSpect 5.1.0 (2019), relativistic spectroscopy DFT program of authors M. Repisky, S. Komorovsky, V. G. Malkin, O. L. Malkina, M. Kaupp, K. Ruud, with contributions from R. Bast, R. Di Remigio, U. Ekstrom, M. Kadek, S. Knecht, L. Konecny, E. Malkin, I. Malkin Ondik (see http://www.respectprogram.org)
22. Dyall KG (2004) Theor Chem Acc 112(5–6):403. https://doi.org/10.1007/s00214-004-0607-y
23. Dyall KG (2006) Theor Chem Acc 117(4):483. https://doi.org/10.1007/s00214-006-0174-5

24. Becke AD (1988) Phys Rev A 38:3098. https://doi.org/10.1103/PhysRevA.38.3098
25. Lee C, Yang W, Parr RG (1988) Phys Rev B 37(2):785. https://doi.org/10.1103/PhysRevB.37.785
26. Becke AD (1993) J Chem Phys 98(7):5648. https://doi.org/10.1063/1.464913
27. Vosko SH, Wilk L, Nusair M (1980) Can J Phys 58:1200. https://doi.org/10.1139/p80-159
28. Stephens PJ, Devlin FJ, Chabalowski CF, Frisch MJ (1994) J Phys Chem 98(45):11623. https://doi.org/10.1021/j100096a001
29. Perdew JP, Burke K, Ernzerhof M (1996) Phys Rev Lett 77:3865. https://doi.org/10.1103/PhysRevLett.77.3865
30. Adamo C, Barone V (1999) J Chem Phys 110(13):6158. https://doi.org/10.1063/1.478522
31. Visscher L (1997) Theor Chem Acc 98:68. https://doi.org/10.1007/s002140050280
32. Barros CL, de Oliveira PJP, Jorge FE, Neto AC, Campos M (2010) Mol Phys. https://doi.org/10.1080/00268976.2010.499377
33. Camiletti GG, Machado SF, Jorge FE (2008) J Comput Chem https://doi.org/10.1002/jcc.20996
34. Neto AC, Jorge FE (2013) Chem Lett Phys https://doi.org/10.1016/j.cplett.2013.07.045
35. DIRAC, a relativistic ab initio electronic structure program, Release DIRAC18 (2018), written by T. Saue, L. Visscher, H. J. Aa. Jensen, and R. Bast, with contributions from V. Bakken, K. G. Dyall, S. Dubillard, U. Ekström, E. Eliav, T. Enevoldsen, E. Faßhauer, T. Fleig, O. Fossgaard, A. S. P. Gomes, E. D. Hedegård, T. Helgaker, J. Henriksson, M. Iliaš, Ch. R. Jacob, S. Knecht, S. Komorovský, O. Kullie, J. K. Lærdahl, C. V. Larsen, Y. S. Lee, H. S. Nataraj, M. K. Nayak, P. Norman, G. Olejniczak, J. Olsen, J. M. H. Olsen, Y. C. Park, J. K. Pedersen, M. Pernpointner, R. di Remigio, K. Ruud, P. Sałek, B. Schimmelpfennig, A. Shee, J. Sikkema, A. J. Thorvaldsen, J. Thyssen, J. van Stralen, S. Villaume, O. Visser, T. Winther, and S. Yamamoto (available at https://doi.org/10.5281/zenodo.2253986, see also http://www.diracprogram.org)
36. Gaussian 09, Revision C.01, M. J. Frisch, G. W. Trucks, H. B. Schlegel, G. E. Scuseria, M. A. Robb, J. R. Cheeseman, G. Scalmani, V. Barone, G. A. Petersson, H. Nakatsuji, X. Li, M. Caricato, A. Marenich, J. Bloino, B. G. Janesko, R. Gomperts, B. Mennucci, H. P. Hratchian, J. V. Ortiz, A. F. Izmaylov, J. L. Sonnenberg, D. Williams-Young, F. Ding, F. Lipparini, F. Egidi, J. Goings, B. Peng, A. Petrone, T. Henderson, D. Ranasinghe, V. G. Zakrzewski, J. Gao, N. Rega, G. Zheng, W. Liang, M. Hada, M. Ehara, K. Toyota, R. Fukuda, J. Hasegawa, M. Ishida, T. Nakajima, Y. Honda, O. Kitao, H. Nakai, T. Vreven, K. Throssell, J. A. Montgomery, Jr., J. E. Peralta, F. Ogliaro, M. Bearpark, J. J. Heyd, E. Brothers, K. N. Kudin, V. N. Staroverov, T. Keith, R. Kobayashi, J. Normand, K. Raghavachari, A. Rendell, J. C. Burant, S. S. Iyengar, J. Tomasi, M. Cossi, J. M. Millam, M. Klene, C. Adamo, R. Cammi, J. W. Ochterski, R. L. Martin, K. Morokuma, O. Farkas, J. B. Foresman, and D. J. Fox, Gaussian, Inc., Wallingford CT, 2016
37. Andrae D, Häußermann U, Dolg M, Stoll H, Preuß H (1990) Theor Chim Acta 77(2):123. https://doi.org/10.1007/BF01114537
38. Yanai T, Tew DP, Handy NC (2004) Chem Phys Lett 393(1):51. https://doi.org/10.1016/j.cplett.2004.06.011
39. Boys S, Bernardi F (1970) Mol. Phys. 19(4):553. https://doi.org/10.1080/00268977000101561
40. Repiský M, Komorovský S, Malkina OL, Malkin VG (2009) Chem Phys 356(1–3):236. https://doi.org/10.1016/j.chemphys.2008.10.037
41. Komorovský S, Repiský M, Malkina OL, Malkin VG, Ondík IM, Kaupp M (2008) J Chem Phys 128(10):104101. https://doi.org/10.1063/1.2837472
42. Komorovský S, Repiský M, Malkina OL, Malkin VG (2010) J Chem Phys 132(15):154101. https://doi.org/10.1063/1.3359849
43. van Duijneveldt FB, van Duijneveldt-van de Rijdt JGCM, van Lenthe JH (1994) Chem Rev 94(7):1873. https://doi.org/10.1021/cr00031a007